
EFFECT OF HEAT TREATMENT AND CROSS SECTION ON THE CRASHWORTHINESS OF 51CRV4 SPRING STEEL

*Çiğdem DİNDAR**
*Hüseyin BEYTÜT***
*Selçuk KARAGÖZ**

Received: 01.11.2018 ; revised: 17.05.2019 ; accepted: 22.07.2019

Abstract: In this study, 51CrV4 spring steel was used as a crash box material and its crashworthiness was investigated under axial dynamic loading. Crash boxes with cylinder and square geometries were designed in SolidWorks and crash analyses were performed by using RADIOSS/explicit and nonlinear Finite Element (FE) codes. In addition, 51CrV4 spring steel was subjected to three different heat treatments and their mechanical properties were determined by tensile and hardness tests. The crashworthiness of crash box was evaluated taking into account the energy absorption (EA), peak crushing force (PCF), mean crushing force (MCF) and crash force efficiency (CFE). Since the crash boxes had equal mass, their EA rates are equal to specific energy absorption (SEA) rates. It has been observed that heat treatment and cross-section geometry have a serious impact on crashworthiness.

Keywords: Crash box, Thin-Walled Tubes, Crashworthiness, Mechanical Strength

51CrV4 Yay Çeliğinde Isıl İşlem ve Kesit Geometrisinin Çarpışma Dayanıklılığı Üzerine Etkisi

Öz: Bu çalışmada, 51CrV4 yay çeliği çarpışma kutusu malzemesi olarak kullanılmış ve çarpışma dayanıklılığı araştırılmıştır. Kare ve silindir kesit geometrisine sahip çarpışma kutuları SolidWorks programında tasarlanmış ve RADIOSS açık zaman entegrasyon yöntemi ve lineer olmayan sonlu elemanlar kodları ile çarpışma analizleri gerçekleştirilmiştir. Buna ek olarak, 51CrV4 çelik malzemesi 3 farklı ısıl işleme maruz bırakılarak mekanik özellikleri çekme ve sertlik testleri ile belirlenmiştir. Belirlenen mekanik özelliklere sahip yapının çarpışma dayanıklılığı, emilen enerji, maksimum çarpışma kuvveti, ortalama çarpışma kuvveti, çarpışma kuvveti verimi dikkate alınarak değerlendirilmiştir. Çarpışma kutularının kütleleri eşit olduğundan emilen enerji oranları özgül enerji emilim oranlarına eşittir. Isıl işlem uygulamasının ve kesit geometrisinin çarpışma dayanıklılığı üzerinde ciddi bir etkisi olduğu gözlemlenmiştir.

Anahtar Kelimeler: Çarpışma Kutusu, İnce-Cidarlı Tüpler, Çarpışma Dayanıklılığı, Mekanik Dayanım,

1. INTRODUCTION

With the increase in the number of vehicle in our country and in the world, accident rates are increasing. This situation forced automotive manufacturers to take new measures. Many security systems have been developed by automotive designers in order to ensure safe transportation of vehicles in traffic. These security systems can be examined under two main

* Bursa Technical University, Faculty of Engineering and Natural Sciences, Mechanical Engineering, 16330. Yıldırım, Bursa

** Bitlis Eren University, Faculty of Engineering and Architecture, Mechanical Engineering, 13100. Merkez, Bitlis

Corresponding Author: Selçuk KARAGÖZ (selcuk.karagoz@btu.edu.tr)

groups as active and passive security systems. While active safety systems reduce the likelihood of an accident happen, passive safety systems allow passengers to circumvent the accident with minimum damage in the event of accident.

Crash box is one of the most important passive safety system member. Therefore, the design of the crash boxes and the choice of materials is extremely critical for passengers and goods safety (Öztürk and Kaya, 2008). The following Figure 1 shows the crash boxes and bumper beam assemble.

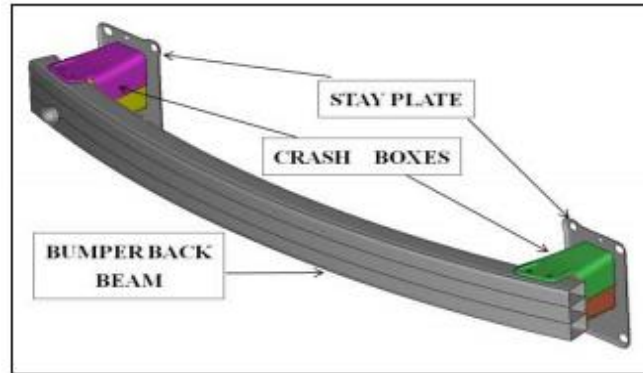


Figure 1:
The assembly of crash box (N Nasir, 2015)

In case of frontal crash accident, the crash box is expected to be collapsed with absorbing kinetic energy of vehicle by undergo plastic deformation, especially at medium and low speeds. In this way, passengers, cargo and critical parts of the vehicle will avoid the accident with minimum damage (Nakazawa at. al., 2005).

Thin-walled structures (TWTs) have a wide range of use in automobiles due to their high energy absorption, easy formability and low cost. Many studies have been focus on increase specific energy absorption of this structure (Xie at. al., 2017; Yıldız at. al., 2016; Karagöz and Yıldız, 2017). The effects of cross-section on crashworthiness have been investigated by using geometries such as square, cylinder, hexagons (Alavi and Parsapour, 2014; Yao at. al., 2017; Liang at. al., 2017). Since the mechanical properties of the materials change by heat treatment applications, it is expected that the crashworthiness of structure will change. In the literature, studies have been carried out on how crashworthiness of the structure changed after heat treatment (Bambach at. al., 2016; Campana and Pilone, 2009; Millett at. al., 2004; Conrads at. Al., 2017).

While determining the crashworthiness of energy absorbers, energy absorption, specific energy absorption, peak crushing force, mean crushing force, and crush for efficiency should be taken into consideration (Tran at. al., 2015).

1.1 Energy Absorption (EA)

What is expected from the crash box is to convert the kinetic energy into plastic deformation energy. EA could be found by the area under the crash load versus displacement curve (Equation 1).

$$EA = \int_0^d P(x)dx \quad (1)$$

Where; P(x) is the axial load, d is the crash distance

1.2 Specific Energy Absorption (SEA)

Specific energy absorption (SEA) is used to indicate the amount of energy absorbed per unit mass of the crash box (Equation 2). So it is important for lightweight design.

$$SEA = \frac{EA}{m} \quad (2)$$

Where; m is the mass of the crash box.

1.3 Peak Crushing Force (PCF)

Studies have shown that the PCF (P_{max}) is generally occurs at the first reaction force (TrongHhan at. Al., 2015). It was observed that the PCF was reduced by adding trigger mechanism (hole, groove etc.) to the crash box (Nasir at. al., 2017).

1.4 Mean Crushing Force (MCF)

The MCF (P_o) is obtained by dividing EA to the crash distance (Equation 3). In terms of energy absorption, crash loads should be stable and close to the MCF.

$$P_o = \frac{EA}{d} \quad (3)$$

1.5 Crush Force Efficiency (CFE)

The CFE (η) is found by the ratio of the MCF to the PCF (Equation 4). Since it depends on both the EA and the PCF, it is an important parameter in evaluating the crashworthiness of the structure.

$$\eta = \frac{P_o}{P_{max}} \quad (4)$$

2. MATERIAL AND METHOD

In this study, 51CrV4 steel was used for the material of crash box. 51CrV4 steel is a spring steel material from the medium carbon steel group. The carbon ratios of the spring steels are the higher than the structural steels, and they are also lower than the carbon ratios of the tool steels. It is important that the ratio of the yield limit to the tensile strength is high and the modulus of elasticity is stable in spring steels.

51CrV4 can be easily heat treated such as austenitizing, quenching and then tempering. In this paper, it has been investigated how to effect on the crashworthiness of material properties such as ductility and strength that can be changed by heat treatment.

2.1 Heat treatment Application

Heat treatment was applied to the material in order to observe both differences the plastic deforming ability and the strength values of spring steel 51CrV4. Thus, the changes in the mechanical properties of the materials by heat treatment were examined and these new mechanical properties were used in the crash analyses.

In the heat treatment process, the tempering temperature was changed. In addition, the austenitizing temperature and duration, cooling temperature in oil were kept constant. The heat treatment application values have showed in Table 1.

Table 1. Heat treatment application parameters

Sample No	Austenitizing Temperature /Duration	Cooling in Oil Temperature	Tempering Temperature /Duration
Sample 1	850°C /1 hour	80°C	400°C /75min
Sample 2	850°C /1 hour	80°C	440°C /75min
Sample 3	850°C /1 hour	80°C	480°C /75min

Primarily, the samples were preheated at 400 ° C for 1 hour in tempering furnaces. When the materials at room temperature had been put to the curing oven placed at temperatures between 850 - 950°C are heated suddenly, the dimensional tolerance change (waste) may be higher than the prescribed values. In addition, the materials can be cracked due to thermal shock and high stress in the curing oven. The base purpose of pre-heating process is to prevent all these predictable errors like thermal shock and high stress.

In preheating processes performed at temperatures higher than 400°C, oxide layer or decarburisation in surface may occur due to the atmosphere-free furnace. Therefore, temperatures in the preheating are generally kept between 300 and 400°C.

After preheating process, austenitization and hardening application of heat treatment had been performed. The austenitization process is applied on the Fe – Fe₃C diagram at approximately 30 - 50 °C above the A3 curve. At the end of the process, austenite phase (face centred cubic structure) is formed in the material. Following the austenitizing process, the steels cooled in a normal air conditions have been normalized. Thus, the material is provided a thinner and homogeneous structure.

The material can be hardened in the result of cooling with air or N₂ and with oil, water or polymer cooling according to the amount of carbon and alloying elements of the steel. The steel in the face centred cubic (FCC) phase is transformed into body centred tetragonal (BCT) martensite phase without diffusion by the sudden cooling process.

In this study, austenitization process was applied to the low alloy steel 51CrV4 at 850°C for 1 hour and then cooled in oil at 80°C. After cooling process in the oil, martensite phase was formed and hardness values of 60 HRC were detected subsequent to the hardness measurement.

Samples dipped to the cooling oil were washed with special chemicals at temperatures among 60 - 80°C. Thus, the oil layers on the surface of the material were cleaned.

In a result of the oil hardening process, the steel in the martensite crystal structure is a very fragile. In order to increase the toughness of the material and to remove the stresses occurring in the structure after the phase transformation, tempering process is applied. Tempering process was carried out at 400°C, 440°C and 480°C for 75 min. As a result of this tempering process, the tension of the material was removed, toughness and ductility values are increased, while the strength and hardness values decrease.

2.2 Mechanical Properties

The most commonly used tests for determining the mechanical strength of materials are hardness and tensile tests. Mechanical properties such as yield strength, tensile strength, modulus of elasticity, elongation at break, fracture energy can be determined by tensile test while hardness measurement provide information about hardness of material. While measurements is performed, it is very important that the precision measurement of data. The samples of the tensile test with each similar parameter has been repeated by three times due to provide the sensitivity of the accuracy of the test. In addition, the hardness of samples which were applied heat treatment had been measured by Rockwell hardness measuring device.

The steels manufactured from 51CrV4 material that we studied in this paper are preferred commonly for anti-roll bar. These steels generally are used in the range 42-48 HRC hardness.

The performance expected from anti-roll bar by 51CrV4 is high yield strength, the material can be sprung and not broken in a short time. However, the fatigue performance of the material is also extremely important. Therefore, when hardness groups are selected in the study, it is considered that the material will be broken when the material is crushed at very low or very high hardness values are reached.

According to results of heat treatment, for the purpose of determine the mechanical properties of material at various hardness values, the samples used in the range 42 - 48 HRC were separated into three hardness groups and the hardness measure tests were carried out. Hardness measurement results are given in Table 2.

Table 2. Range of hardness groups according to tempering temperatures

	Tempering Parameters and Hardness Measurements
Group of 46-48 HRC	400°C - 75 min tempering after curing. The measured hardness value is 48 HRC
Group of 44-46 HRC	440°C - 75 min tempering after curing. The measured hardness value is 45 HRC
Group of 42-44 HRC	480°C - 75 min tempering after curing. The measured hardness value is 43 HRC

The graph of Rockwell hardness values measured with varying temperature is shown in Figure 2. The hardness values decreased as tempering temperature increased.

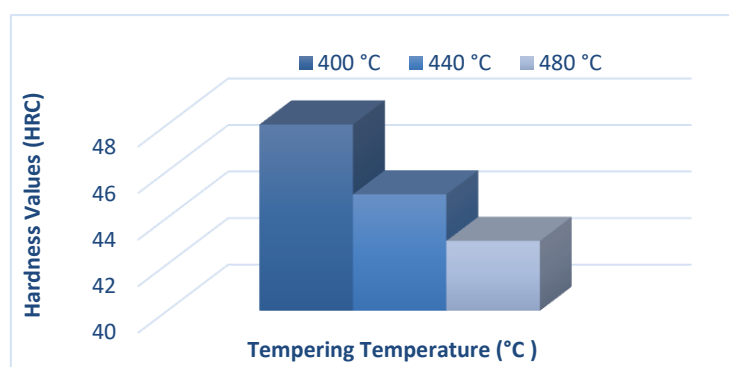


Figure 2:
Hardness values after tempering temperature

After the hardness test, the mechanical properties of the samples were determined by tensile tests. Heat treated samples was prepared according to TS 138A norm, such that dimensions are thickness (t) is 1.93 mm, width (b) is 5.9 mm and length (L_0) is 32 mm. A tensile test was applied to samples in the given dimensions with the test machine given at a single axis, at a strain rate of 10^{-3} s^{-1} and at the constant room temperature. For the accuracy of each parameter, samples were tested three times and in total, twelve tensile samples because of four different process parameters were tested. Following Figure 3 shows tensile test machine and samples. The result of the samples after tensile test are given in Figure 4.



Figure 3:
The tensile test machine and the samples

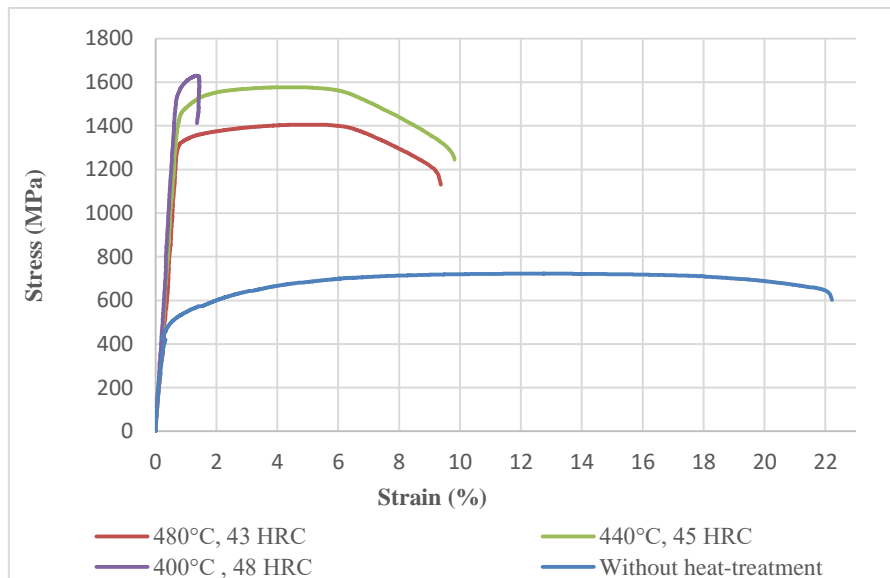


Figure 4:
True stress-strain curve after heat-treatment

2.3 Crash Analysis

For crash analysis, design of the crash box was carried out after the mechanical properties of the heat-treated material to be used in the analysis were determined by hardness and tensile tests. Crash box to be used in analysis is designed in SolidWorks software. Pre-processing was performed by using HyperCrash, RADIOSS/explicit was used as a solver and for post-processing HyperGraph and HyperView were utilized. Process methodology of crash analysis has been shown in Figure 5.

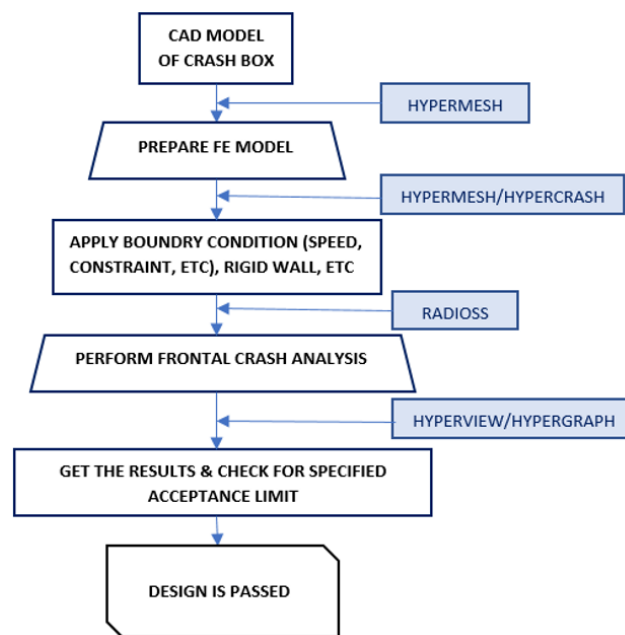


Figure 5:
Process methodology of the crash analysis

Crash analyses have been carried out in two different types of crash box as square and cylindrical cross sections. The perimeter of the cross sections for cylindrical and square crash boxes were 360 mm, the length is 130 mm and wall thickness is 1.2 mm. In this way, the masses of the crash boxes are ensured to be equal. 3 mm x 3 mm mesh size was utilized. The velocity of the was preferred 13.89 m/s that is taken from EURO NCAP protocol and 600 kg mass was added to end of the crash box. The total kinetic energy of the model was 57880 J. “Nodes to Surface Contact” definition was utilized with 0.2 friction coefficient between the crash box and rigid wall and self-contact algorithm is used for avoiding interpenetration between crash box surface during folding, provided by RADIOSS. For avoiding hourglass energy 5 integration point used through the thickness. The crash box is restricted to all degrees of freedom except for the axis of speed x.

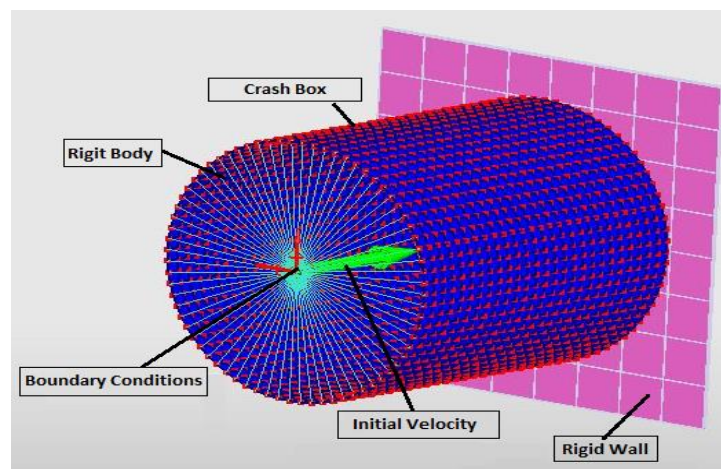


Figure 6:
Finite element model of crash box before crash analysis

3. RESULTS AND DISCUSSION

Explicit and non-linear analyses of the crash boxes were performed and the crash force-displacement and absorbed energy-displacement curves were obtained (Figure 7 and 8).

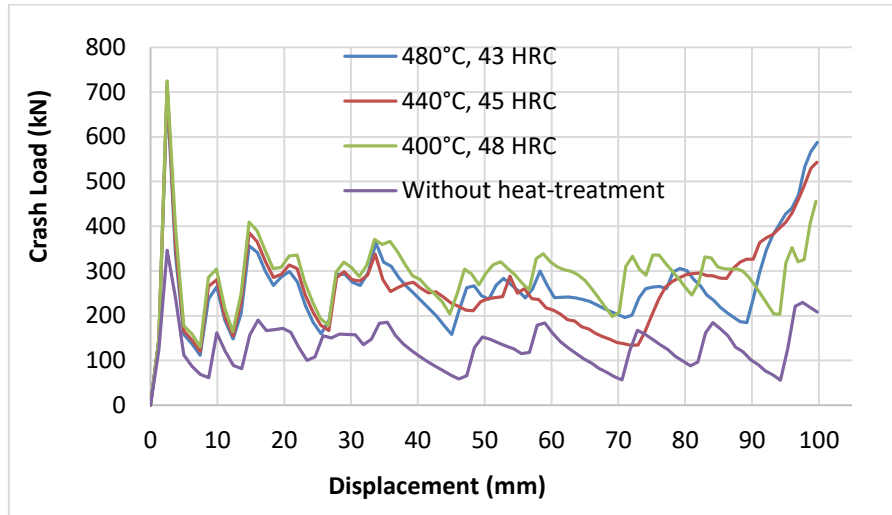


Figure 7:
Crash load versus displacement curve for cylinder tube

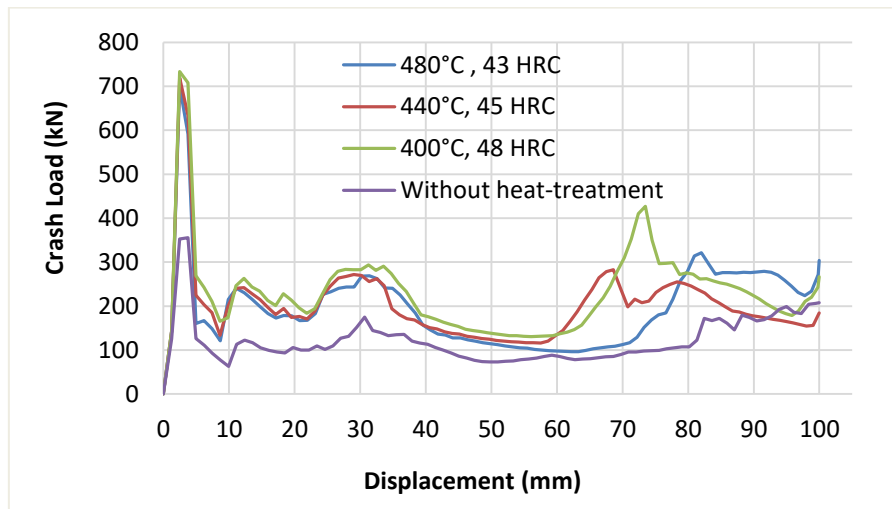


Figure 8:
Crash load versus displacement curves for square tube

As shown in Figure 7 and 8, the crash loads of the cylindrical crash box were more stable than the square crash box. Since the strength of the material was increased after the heat treatment application, the first folding was occurred difficult and therefore the PCF was higher for both geometries. While The PCF of the non-heat-treated crash boxes were the lowest, the crash boxes subjected to heat treatment at 400°C were the highest. Absorbing energy versus displacement curve of cylindrical and square crash boxes were given in Figure 9 and Figure 10, respectively.

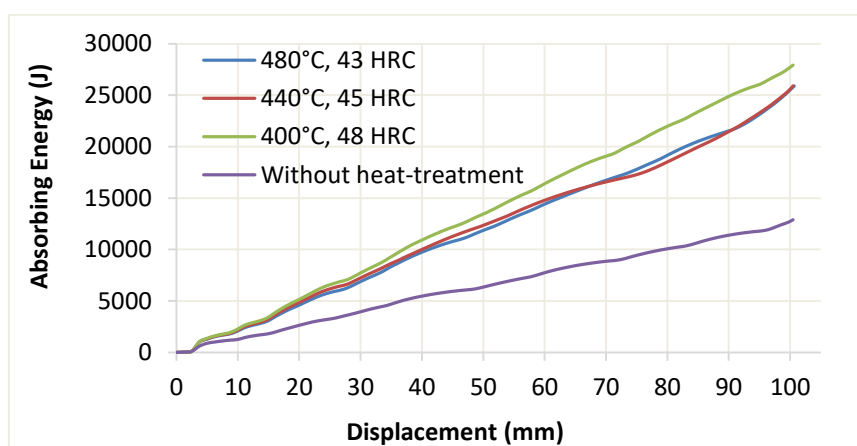


Figure 9:
Absorbing energy-displacement graph for cylinder tube

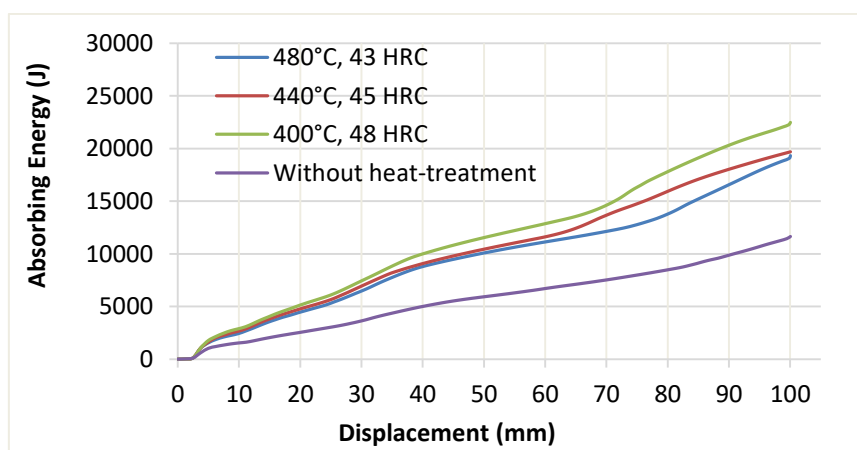


Figure 10:
Absorbing energy-displacement graph for square tube

The impact response of the cylindrical and square crash boxes after heat treatment are given in Table 3. Since The crash boxes had equal mass, their energy absorption rates equal to their specific energy absorption. In all cases, EA, MCF and CFE of the cylindrical crash boxes were higher than the square crash boxes. When the crashworthiness of the crash boxes was evaluated in terms of CFE, the best result was obtained at 400°C heat-treated cylindrical crash box, while the worst result obtained at 440°C heat-treated square crash box. With parallel to literature, crashworthiness of cylindrical crash box was better than square crash box.

Table 3. Impact response of the cylindrical and square crash boxes

Condition	Without heat treatment				400°C heat treatment			
	AE (J)	PCF (kN)	MCF (kN)	CFE	AE (J)	PCF (kN)	MCF (kN)	CFE
Cylinder	12671	347	126.9	0.366	27928	725	279.9	0.386
Square	11648	353	116.7	0.33	22482	733	225.2	0.307
Condition	440°C heat treatment				480°C heat treatment			
	AE (J)	PCF (kN)	MCF (kN)	CFE	AE (J)	PCF (kN)	MCF (kN)	CFE
Cylinder	25426	713	254.82	0.357	25375	694	254.31	0.366
Square	19869	719	199.03	0.277	19464	701	194.97	0.278

CONCLUSION

In this study, the effect of heat treatment on crashworthiness of 51CRV4 spring steel was investigated. Therefore, the 51CRV4 spring steel has been subjected to three different heat treatments (400°C 440°C and 480°C). After heat treatment the mechanical properties of heat-treated 51CRV4 spring steel were determined by tensile and hardness tests. In addition, cylindrical and square collision boxes were designed to investigate the impact of cross-section on crashworthiness. Accordingly, the following conclusions can be drawn.

- Since the mechanical properties of 51CRV4 spring steel changed after the heat treatment, the crash performance also changed. It has been concluded that the application of heat treatment has a serious effect on the crash performance.
- The EA of the cylindrical box which subjected to the heat treatment at 400°C increased by 120.4% and PCF increased by 108.9%. For square crash box, EA increased by 93% and PCF increased by 107.6%
- The cross-section had a serious effect on the crash performance. The crashworthiness of the cylindrical crash box was better for all cases.
- In all cases, the PCF of the cylindrical crash box was lower than the square crash box and subsequent crash loads were. more stable

ACKNOWLEDGEMENTS

Thanks to the ÖNERLER Company for the heat treatment applications.

REFERENCES

1. Alavi Nia, A. and Parsapour, M. (2014). Comparative analysis of energy absorption capacity of simple and multi-cell thin-walled tubes with triangular, square, hexagonal and octagonal sections. *Thin-Walled Structures*, 74, 155-165. doi:10.1016/j.tws.2013.10.005.
2. Bambach, M., Conrads, L., Daamen, M., Güvenç, O, and Hirt, G. (2016). Enhancing the crashworthiness of high-manganese steel by strain-hardening engineering, and tailored folding by local heat-treatment. *Materials & Design*, 110, 157-168. doi:10.1016/j.matdes.2016.07.065.
3. Campana, F. and Pilone, D. (2009). Effect of heat treatments on the mechanical behaviour of aluminium alloy foams. *Scripta Materialia*, 60(8), 679-682. doi:10.1016/j.scriptamat.2008.12.045.
4. Conrads, L., Conrad, L. and Hirt G. (2017). Increasing the energy absorption capacity of structural components made of low alloy steel by combining strain hardening and local heat treatment. *International Conference on the Technology of Plasticity*, ICTP 2017, 17-22 September 2017, Cambridge, United Kingdom. doi: 10.1016/j.proeng.2017.10.771
5. Karagöz, S. and Yıldız, A. R. (2017). Comparison of recent metaheuristic algorithms for crashworthiness optimisation of vehicle thin-walled tubes considering sheet metal forming effects. *Int. J. Vehicle Design*, Vol. 73, Nos. 1/2/3, 2017. doi:10.1504/IJVD.2017.082593
6. Liang, C., Wang, C. J., Nguyen, V. B., English, M. and Mynors, D. (2017). Experimental and numerical study on crashworthiness of cold-formed dimpled steel columns. *Thin-Walled Structures*, 112, 83-91. doi:10.1016/j.tws.2016.12.020.
7. Millett, J., Bourne, N. and Edwards, M. (2004). The effect of heat treatment on the shock induced mechanical properties of the aluminium alloy, 7017. *Scripta Materialia*, 51(10), 967-971. doi:10.1016/j.scriptamat.2004.07.020.

8. Nakazawa, Y., Tamura, K., Yoshida, M., Tagaki, K. and Kano, M. (2005) Development of crash-box for passenger car with high capability for energy absorption, *VIII. International Conference on Computational Plasticity*, Barcelona, Spain.
9. N Nasir, H., Srinivasa Prakash, R., Yendluri V. and Daseswara, R. (2017). Comparative Study Of Trigger Configuration For Enhancement Of Crashworthiness Of Automobile Crash Box Subjected To Axial Impact Loading. *Procedia Engineering*, 173, 1390-1398. doi: 10.1016/j.proeng.2016.12.198
10. N Nasir, H. (2015). Automobile Crash Box Design Improvement Using HyperStudy. India *Altair Technology Conference. Hyundai Motor India Engineering Pvt. Ltd.* Survey No. 5/2,5/3. Opp. Hitech City Railway Station, Izzatnagar, Hyd – 84.
11. Öztürk, İ. and Kaya, N. (2008). Otomobil Ön Tampon Çarpışma Analizi Ve Optimizasyon, *Uludağ Üniversitesi Mühendislik-Mimarlık Fakültesi Dergisi*, Cilt 13, Sayı 1.
12. Tran, T., Hou, S., Han, X. and Chau, M. (2015). Crushing analysis and numerical optimization of angle element structures under axial impact loading. *Composite Structures*, 119, 422-435. doi:10.1016/j.compstruct.2014.09.019.
13. Xie, S., Yang, W., Wang, N. and Li, H. (2017). Crashworthiness analysis of multi-cell square tubes under axial loads. *International Journal of Mechanical Sciences*, 121, 106-118. doi:10.1016/j.ijmecsci.2016.12.005.
14. Yao, S., Xing, Y. and Zhao, K. (2017). Crashworthiness analysis and multiobjective optimization for circular tubes with functionally graded thickness under multiple loading angles. *Advances in Mechanical Engineering*, 9(4). doi:10.1177/1687814017696660.
15. Yıldız, A. R., Kurtuluş, E., Demirci, E., Yıldız, B. S. and Karagöz, S. (2016). Optimization of thin-wall structures using hybrid gravitational search and Nelder-Mead algorithm. *Materials Testing*, Vol. 58, No. 1, pp. 75-78. <https://doi.org/10.3139/120.110823>.

